

MANGANESE-RICH GARNET ROCKS ASSOCIATED WITH THE BROKEN HILL LEAD-ZINC-SILVER DEPOSIT, NEW SOUTH WALES, AUSTRALIA

PAUL G. SPRY AND J. DAVID WONDER*

Department of Geological and Atmospheric Sciences, 253 Science I, Iowa State University, Ames, Iowa 50011, U.S.A.

ABSTRACT

Rocks rich in manganian garnet are spatially and genetically related to metamorphosed sulfide deposits and represent exploration guides. At the Broken Hill Pb-Zn-Ag deposit, New South Wales, Australia, three varieties of garnet-rich rock are found at wallrock margins or as blocks within ore. These three rock types can be distinguished either on the basis of mineralogy or by their genetic relationship to features of prograde or retrograde deformation. Quartz-bearing garnetite, the most abundant garnet-rich rock type, contains up to 80% garnet and can be divided into at least seven subtypes on the basis of mineralogy. Garnetite contains between 80% and 95% garnet and occurs on the margins of the Lead lodes and as blocks in the A lode. Layering in quartz-bearing garnetite and garnetite is concordant to a schistosity that formed in the surrounding country-rock during a prograde metamorphic event. "Garnet envelope", a narrow zone of garnet-rich rock at orebody margins, is variable, from discordant to a prograde schistosity, or is concordant to a retrograde schistosity in the wallrocks, or it surrounds late-stage quartz-fluorite veins. The precursors to quartz-bearing garnetite and garnetite formed when Mn-rich emanations from hydrothermal hot springs mixed with pelagic clays and were subsequently metamorphosed. Patterns of garnet zonation and structural relationships suggest that "garnet envelope" was produced during a retrograde metamorphic event by the reaction of fluids from the ore horizon and Al-rich wall rocks. Calculation of equilibria between aqueous solutions and Fe and Mn minerals at ore-forming temperatures reveals that Fe oxides and sulfides are stable at lower oxidation potentials than Mn minerals. A model for mixing of a hydrothermal solution and seawater demonstrates that Fe minerals normally precipitate from solution before Mn minerals, regardless of the nature of the aqueous species present. This fractionation of Fe and Mn can be used to explain the increase in Mn/Fe from the stratigraphic foot-wall relative to the hanging wall of the Broken Hill deposit.

Keywords: manganian garnet rocks, Broken Hill, Australia, massive sulfides, whole-rock analyses, electron-microprobe data, Fe-Mn fractionation.

SOMMAIRE

Des roches riches en grenat manganifère sont associées, tant dans l'espace que dans le temps, aux gisements de sulfures métamorphisés, et représentent ainsi des guides utiles pour l'exploration de ceux-ci. A Broken Hill (New South Wales, en Australie), gisement de Pb-Zn-Ag, nous distinguons trois variétés de "grenatite" situés tout près des roches encaissantes ou au sein des amas de minerai au moyen des assemblages minéralogiques et des signes de déformation rétrograde. La grenatite quartzifère, la plus abondante, peut contenir jusqu'à 80% de grenat, et comprend au moins sept sous-types différenciables par critères minéralogiques. La grenatite, qui contient entre 80 et 95% de grenat, caractérise les bordures des zones minéralisées en plomb, et forme aussi des enclaves dans la zone A. Un rubanement dans la grenatite quartzifère et la grenatite est conforme à la schistosité qui marque un événement métamorphique prograde dans les roches encaissantes. Une étroite enveloppe riche en grenat à la limite des zones minéralisées présente un aspect assez variable; elle est discordante par rapport au plan de schistosité prograde ou concordante avec le plan de schistosité rétrograde, ou elle entoure les fissures à quartz-fluorite tardives. La grenatite quartzifère et la grenatite représenteraient des précipités manganifères issus des événements hydrothermaux auxquels ont été mélangés des argiles pélagiques, le tout métamorphisé par la suite. La zonation des cristaux de grenat et les relations structurales font penser que l'enveloppe riche en grenat résulte du métamorphisme rétrograde qu'a causé la circulation des fluides de la zone minéralisée dans les roches alumineuses de l'encaissant. Un calcul des équilibres entre solution aqueuse et minéraux riches en Fe et Mn aux températures appropriées pour la formation du minerai montre que les oxydes de fer et les sulfures sont stables à de plus faibles potentiels d'oxydation que les minéraux riches en Mn. Notre modèle de la précipitation anticipée suite à un mélange d'une solution hydrothermale avec de l'eau de mer prédit la formation de minéraux riches en fer normalement avant ceux qui sont enrichis en Mn, quelle que soit la nature des complexes aqueux. Cette séparation du Fe et du Mn expliquerait l'augmentation du rapport Mn/Fe à partir des roches sous-jacentes du gisement de Broken Hill vers les roches stratigraphiquement plus élevées, qui recouvrent celui-ci.

(Traduit par la Rédaction)

Present address: Eugene A. Hickok and Associates, 10550
New York Avenue, Suite C, Des Moines, Iowa 50322,
U.S.A.

Mots-clés: roches riches en grenat manganifère, Broken Hill, Australie, sulfures massifs, données chimiques (roches totales), données par microsonde électronique, fractionnement Fe-Mn.

INTRODUCTION

Garnet-rich rocks, generally manganese-bearing, are associated with a variety of metamorphosed base-metal sulfides at Broken Hill, Australia (Stanton 1976, Barnes *et al.* 1983), Gamsberg, South Africa (Stumpfl 1979, Rozendaal & Stumpfl 1984), Aggeneys, South Africa (Ryan *et al.* 1982), Pegmont, Australia (Vaughan & Stanton 1986) and Mount Misery, Australia (Stanton 1982), gold mineralization at various localities (Valliant & Barnett 1982, Wonder *et al.* 1988) and stibnite mineralization in the Kreuzeck Mountains, Austria (Reimann & Stumpfl 1981). Although quartz-garnet rocks, or cotecules, are commonly associated with these ore deposits, additional minerals form significant petrological variants. Such variants include gahnite-garnet quartzites at Oranjefontein, South Africa (Hicks *et al.* 1985) and Aggeneys, South Africa (Spry 1987), garnet-magnetite-quartz rocks at Gamsberg, South Africa (Rozendaal & Stumpfl 1984), Pegmont (Vaughan & Stanton 1986) and Broken Hill, Australia (Stanton 1976) and in western Georgia (Wonder *et al.* 1988), garnet-quartz-biotite rocks at Pegmont (Vaughan & Stanton 1986), and garnet-quartz-muscovite rocks at Bousquet, Quebec (Valliant & Barnett 1982).

Jacquet (1894) described a garnet-quartz rock and a friable garnet rock at the margins of the Broken Hill deposit and named them "garnet quartzite" and "garnet sandstone", respectively. The widely discussed genetic relationship of these rocks to the deposit has resulted in a variety of interpretations, including: 1) derivation from manganese-bearing chemical sediments (Richards 1966, Stanton 1976, Billington 1979, Spry 1979), (2) isochemical metamorphism of an original manganese-bearing sediment (Segnit 1961, Haydon & McConachy 1987), and (3) relationship to either ore-forming solutions or to metasomatic interaction between the deposit and the wallrocks (*e.g.*, Henderson 1953, O'Driscoll 1953, Stillwell 1959). Hodgson (1975) and Lee (1977) considered that this metasomatic interaction occurred during a high-grade metamorphic event.

The term "garnet rim" was introduced by Jones (1968) for narrow zones, 1 to 50 cm wide, formed of orange-brown garnet and quartz that occur intermittently along the contacts of the orebody and that are discordant to a high-grade schistosity in the adjacent wallrocks. Jones suggested that "garnet rim" and "garnet sandstone" formed by metasomatic exchange of Mn and Ca between the orebody and the adjacent gneiss during a retrograde metamorphic event. Further descriptions of "garnet rim" have been made by Ransom (1969), Maiden (1972), Hodgson (1975) and Billington (1976). In contrast to Jones (1968), Billington (1976) proposed that "gar-

net rim" formed during a prograde metamorphic event by metasomatic exchange between the orebodies and the wallrocks.

Analyses by Hawkins (1968), Stanton *et al.* (1978) and Plimer (1979) have shown that a manganese anomaly is spatially associated with the Broken Hill deposit. The data of Hawkins show that there is a general increase in Mn/Fe from the footwall to the hanging wall of the deposit in the southern end of the field. The absence of data on Fe concentrations in the northern orebodies precludes an accurate determination of the variation of Mn/Fe in individual orebodies along strike. Despite this, the abundance and nature of gangue minerals in the individual orebodies suggest a general increase of Mn/Fe in the orebodies from south to north (Plimer 1979).

The current study attempts to classify various garnet-rich rock types associated with the Broken Hill deposit and to resolve previous conflicts in interpretations of the origin of these rock types. A thermochemical study is used to explain the apparent increase in the ratio Mn/Fe from the stratigraphic footwall to the hanging wall of the deposit. Because of the association of rocks containing manganese-bearing garnet with other sulfide deposits, the exploration potential of these rocks also is discussed.

GEOLOGY OF THE BROKEN HILL DEPOSIT

The Broken Hill deposit occurs in a distinctive suite of rocks of the Purnamoota Subgroup, which forms part of the Broken Hill Group within the Proterozoic Willyama Complex (Willis *et al.* 1983). The Complex is composed of metasediments with minor quartzofeldspathic, basic and ultrabasic rocks (Stevens *et al.* 1980, Willis *et al.* 1983). Although Stevens *et al.* and Willis *et al.* suggested that some of the minor rock types have volcanic precursors, Haydon & McConachy (1987) suggested that they were all sediments originally. The Broken Hill Group consists of metapelites, amphibolites, felsic gneiss, garnet-plagioclase gneiss ("Potosi" gneiss), quartzitic gneiss and lode-horizon rocks (Fig. 1). The last unit consists of garnet-rich rocks ("garnet quartzite", "garnet sandstone" and "garnet rim"), quartz-gahnite lode and lode pegmatite (Johnson & Klingner 1975, Barnes *et al.* 1983). "Garnet quartzite" is the most common garnet-rich rock type and is often not associated with Pb-Zn mineralization (Barnes *et al.* 1983).

The Broken Hill Pb-Zn-Ag orebodies (300 million tons of >5% combined metals) were deposited at about 1,800 Ma and underwent a granulite-grade metamorphic event at about 1,700 Ma (Pidgeon 1967, Shaw 1968). K-Ar and Rb-Sr mineral dates indicate an amphibolite-grade metamorphic event at about 500 Ma (Evernden & Richards 1961, Richards

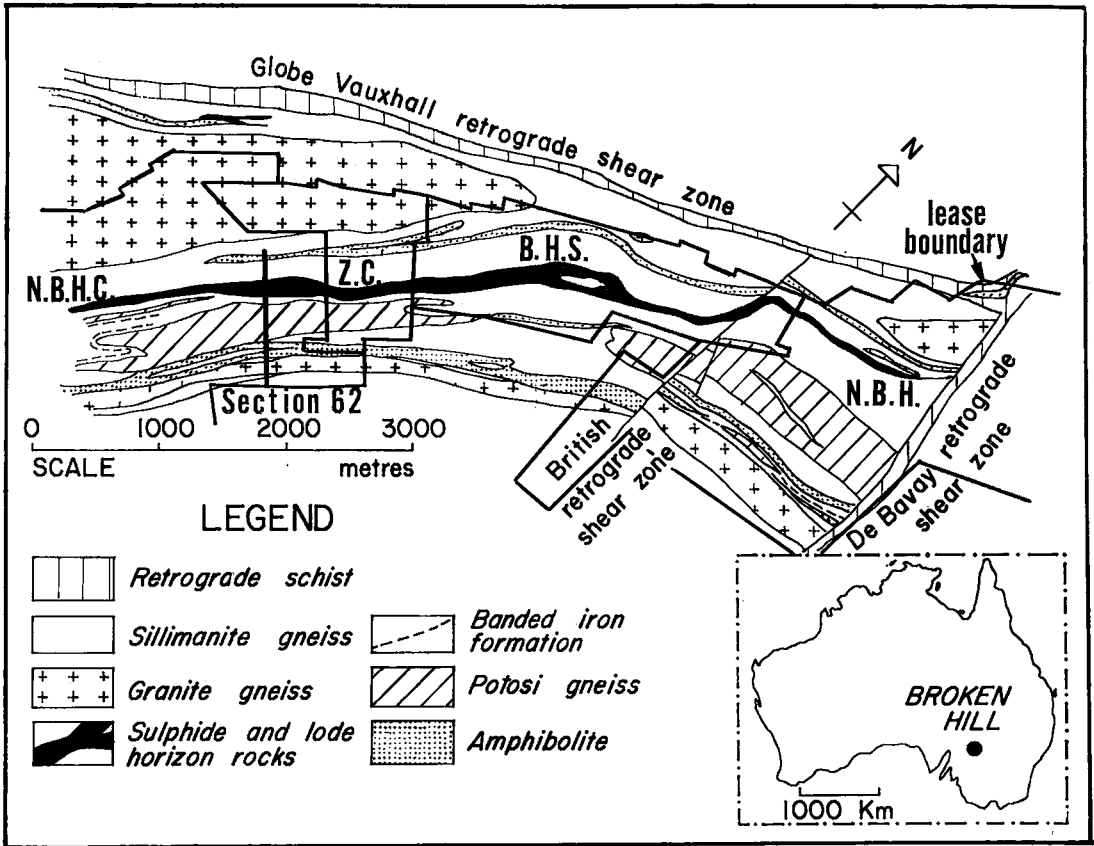


FIG. 1. Geological map of the Broken Hill lode.

& Pidgeon 1963). Structural work by Laing *et al.* (1978) demonstrated four episodes of folding. The mine sequence occurs on a single inverted limb of a first-generation fold, which overturned the orebodies. The lode horizon contains six separate orebodies, each of which has a characteristic gangue mineralogy and base metal content (Plimer 1979). Only in the Zinc Corporation (Z.C.) mine are all six lenses present. In order of stratigraphic succession they are:

Top	3 lens	} Lead lodes
	2 lens	
	1 lens	} Zinc lodes
	A lode	
	B lode	
	C lode	

A cross-section through five of the lenses in the New Broken Hill Consolidated (N.B.H.C.) mine is shown in Figure 2. The C lode occurs as weak stringer-type mineralization in the Z.C. mine. Several intersections of zinc-rich mineralization known as Zinc lode have been exposed by workings at the North Broken Hill (N.B.H.) mine.

Laing *et al.* (1978) considered that the Broken Hill orebodies were deposited at the end of a period of volcanism and were succeeded by a thick unit of nonvolcanogenic sediment (*i.e.*, sillimanite gneiss). Laing *et al.* (1984) proposed the presence of ignimbrites and pumice-fall deposits in the enigmatic Potosi gneiss. However, the identity of these deposits must be questioned since they have been subject to granulite-grade metamorphism. A volcanogenic-exhalative source for the sulfides has been favored by a number of workers (*e.g.*, Stanton & Russel 1959, Plimer 1979, Willis *et al.* 1983), and Both & Rutland (1976) considered that sulfides were deposited when metal-rich saline brines migrated through a sedimen-

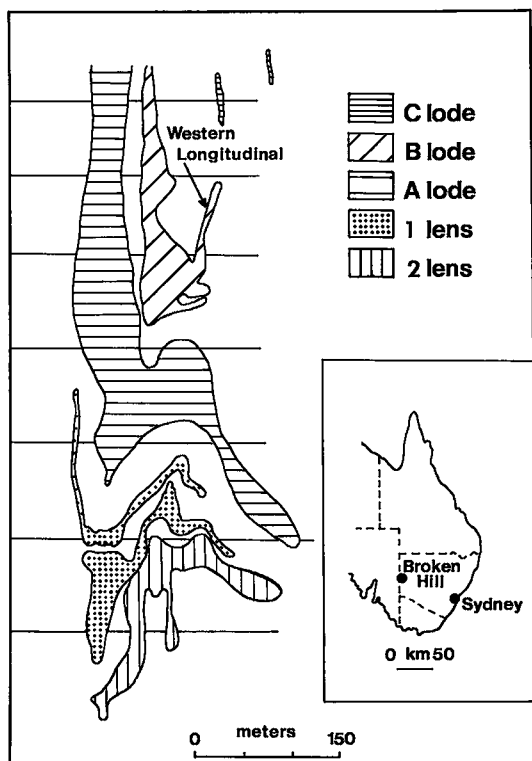


FIG. 2. Cross-section (No. 62) through the New Broken Hill Consolidated mine haulage shaft, looking south 18° east.

tary or volcanic pile onto the floor of a sedimentary basin. Recently, Haydon & McConachy (1987) and Wright *et al.* (1987) suggested that Pb-Zn-Ag mineralization was related to compactive expulsion of metal-bearing brines during accumulation of a thick sedimentary pile. Additional hypotheses suggest that ore fluids were derived from formation waters (Johnson & Klingner 1975), downwardly convected seawater (Russel 1983), and metasomatized mantle (Plimer 1985).

MINERALOGY AND PETROLOGY OF GARNET-RICH ROCKS

lthough we recognize the three garnet-rich rock types at Broken Hill that have been proposed by earlier workers (*e.g.*, Johnson & Klingner 1975), we suggest that the terms "garnet quartzite", "garnet sandstone" and "garnet rim" be replaced by "quartz-bearing garnetite", "garnetite", and "garnet envelope", respectively. Quartz-bearing garnetite with more than 3% of each accessory mineral

is further distinguished by the nature of the accessory minerals. Previous attempts at a classification of the quartz-bearing garnetites were made by Spry (1978) and Billington (1979), but are unsatisfactory because both classification schemes use a combination of structural and mineralogical terms. Furthermore, these authors referred to the rocks as garnet-bearing quartzites, which implies that they were formed by metamorphism of sandstone or chert. As will be discussed later, such precursors are unlikely because of the high Al content of some of the quartz-bearing garnetites. The main characteristics of the seven types of quartz-bearing garnetites are summarized in Table 1.

The term "garnet sandstone" is a misnomer that has been retained in the literature on Broken Hill since it was introduced by Jacquet (1894). The rock is not an unmetamorphosed sandstone as the name implies, but is a friable metamorphic rock in which garnet comprises over 80% by volume. To avoid confusion between a garnet-rich rock-type and the edge of an individual grain of garnet, the term "garnet rim" is considered unsatisfactory for discordant garnet-rich rocks at the edge of orebodies. It is for this reason that the term "garnet envelope" has been introduced. The main characteristics of garnetite and garnet envelope are summarized in Table 2, and the spatial relationship of garnet-rich rock types to the orebodies is shown in Figure 3.

Quartz-bearing garnetite and garnetite contain many of the same minerals and exhibit similar textures. For example, they are commonly massive (Fig. 4a), exhibit a granoblastic texture (Fig. 4b), or are layered. These layers, 2 mm to 10 cm thick and up to 10 m long, are defined by alternations of garnet and sulfide (Fig. 4c), variations in the size and color of garnet, and alternations of garnet with other silicates (Fig. 4d). These layers reflect original compositional banding similar to that present in banded iron formation (Fig. 5a) and sillimanite gneiss adjacent to the lode.

Quartz-bearing garnetite and garnetite are characterized by minerals that were stable during the prograde metamorphic event. These minerals consist of quartz, garnet, biotite, apatite, gahnite, sphalerite, pyrrhotite, plagioclase, orthoclase, hedenbergite, and wollastonite, and commonly exhibit sharp contacts between each other. The most common assemblage is quartz-garnet and quartz-garnet-biotite (Figs. 4a,d). Because of the absence of primary muscovite or K-feldspar in most varieties of quartz-bearing garnetite, it is not possible to represent the prograde assemblages on AFM diagrams. Staurolite (Fig. 5b), cummingtonite, muscovite, talc, pyrite and chlorite cut across grain boundaries and have formed at the expense of prograde assemblages

TABLE 1. CHARACTERISTICS OF QUARTZ-BEARING GARNETITE

	Garnet Content, Grain Size, and Garnet Color	Mineralogy (in approximate order of abundance)	Texture	Relative Abundance	Location
1. Quartz garnetite	up to 80%, 0.1 mm to 1 cm, orange-brown to pink	Qtz, Grt, Bt, Chl ⁺ , Ilm, Gah, Fl, Ap, Pl, Sil, Mus ⁺ , St ⁺ , Hbl ⁺ , Act ⁺ , Cum ⁺ , Gn, Sp, Po, Ccp, Py ⁺ , Mag, Apy, Lo, Hd	massive or layered (rarely cross-cutting)	most abundant type	all lenses, however layered and cross-cutting types most common adjacent Lead lodes
2. Quartz-biotite garnetite	up to 80%, 0.1 to 0.5 mm, orange and pink	Qtz, Bt, Grt, Chl ⁺ , Mus ⁺ , Ap, Cum ⁺ , Gn, Sp, Po, Ccp, Tet, Py ⁺ , Apy, Lo, Nic, Ilm, Gah, (?) Dys	weak foliation	common	all lenses
3. Quartz-gahnite garnetite	20 to 80%, 0.5 to 5 mm, red	Qtz, Grt, Gah, Bt, Chl ⁺ , Po, Sp, Gn, St ⁺ , Mus ⁺ , Ilm	massive	common	all lenses, most common in and around B and C lodes
4. Quartz-sillimanite garnetite	10 to 20%, 0.1 to 0.3 mm, pink	Qtz, Grt, Bt, Sil, Mus ⁺ , St ⁺ , Or, Po, Ilm, Ccp, Sp, Cb, Gn, Apy	layered in places, weak foliation	rare	B lode and 1 lens only
5. Quartz-feldspar garnetite	10 to 20%, 0.1 to 0.2 mm, orange	Qtz, Pl, Or, Grt, Bt, Chl ⁺ , Zo, Sp, Gn, Po, Ccp, Py ⁺	massive	rare	near margins of 2 and 3 lens
6. Quartz-cordierite garnetite*	up to 15%, up to 5 mm, pink	Qtz, Crd, Bt, Mus ⁺ , Grt, Kfs, Chl ⁺ , Tlc ⁺ , Sp, Gn, Ccp, Po, Py ⁺	weakly layered	rare	1 lens and C lode
7. Quartz-muscovite-staurolite garnetite*	up to 50%, up to 0.5 mm, orange-red to pink	Qtz, Mus ⁺ , St ⁺ , Grt, Bt, Gah, Sil, Crd, Wo, Chl ⁺ , Sp, Gn, Ccp, Po, Py	weakly foliated	rare	retrograde shear zones

*After Billington (1979); Act actinolite; Ap apatite; Apy arsenopyrite; Bt biotite; Cb cubanite; Ccp chalcopyrite; Chl chlorite; Crd cordierite; Cum cummingtonite; Dys dyscrasite; Fl fluorite; Gah gahnite; Gn galena; Hbl hornblende; Hd hedenbergite; Ilm ilmenite; Kfs K feldspar; Lo löllingite; Mag magnetite; Mus muscovite; Nic nickeline; Or orthoclase; Pl plagioclase; Po pyrrhotite; Py pyrite; Qtz quartz; Sil sillimanite; Sp sphalerite; St staurolite; Tet tetrahedrite; Tl talc; Wo wollastonite; Zo zoisite, + secondary mineral

TABLE 2. CHARACTERISTICS OF GARNETITE AND GARNET ENVELOPE*

	Garnet Content, Grain Size, and Garnet Color	Mineralogy (in approximate order of abundance)	Texture	Relative Abundance	Location
Garnetite	80-95%, 0.05 to 0.5 mm, orange-brown to pink	Grt, Qtz, Ap, Ti, Chl ⁺ , Bi, Gn, Sp, Lo, Apy, Hd, Mus ⁺ , Cal, Ep, Fl, Afs, Gr (?), Cum ⁺ , Sil, Hbl ⁺ , Ves ⁺ , Sc, Po, Te ⁺ , Ccp, Mar ⁺ , Py ⁺ , Dys, Tro, Mk ⁺ , Bl, Gd, Ilm, Rt, Mag, Hem ⁺ , Gah	granoblastic mosaic of interlocking grains, layered in places	common	margins of, and pods in 1, 2 and 3 lenses and A lode
Garnet envelope	up to 80%, 1 mm to 1 cm, orange-brown	Grt, Qtz, Apy, Zrn, Bt, Mus ⁺ , Chl ⁺ , Ti, Ab, Cum ⁺ , Ep, Hbl, Czo, Hd, Lo, Apy, Py, Mar, Mk, Cub, Sp, Gn, Ccp, Po, Tet	garnet forms in granoblastic mosaic in trains concordant to retrograde schistosity	uncommon	margins of Lead lodes, and surrounding late-stage veins in 2 lens (N.B.H.C.) and Zinc lode (N.B.H.)

Ab albite; Afs alkali feldspar; Bl boulangerite; Cal calcite; Cub cubanite; Czo clinozoisite; Ep epidote; Gr graphite; Hem hematite; Mar marcasite; Rt rutile; Sc scheelite; Ti titanite; Tro troilite; Ves vesuvianite; Zrn zircon; * other mineral abbreviations are listed in Table 1

during a retrograde metamorphic event. The Globe-Vauxhall, British and De Bavay shear zones, which were active during the 500 Ma amphibolite-grade metamorphic event, contain an abundance of these retrograde minerals.

In garnet envelope, garnet characteristically is either discordant to a wallrock schistosity that formed during a prograde metamorphic event, or is present in trains concordant to wallrock schistosity that formed during a retrograde metamorphic event

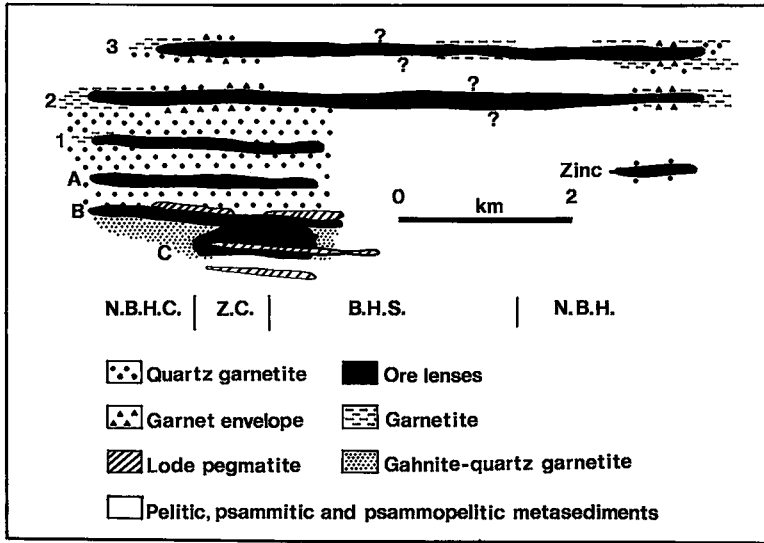


FIG. 3. Schematic reconstruction of the Broken Hill lode showing the spatial relationship of the most abundant garnet-rich rocks to the orebodies (modified from Haydon & McConachy 1987).

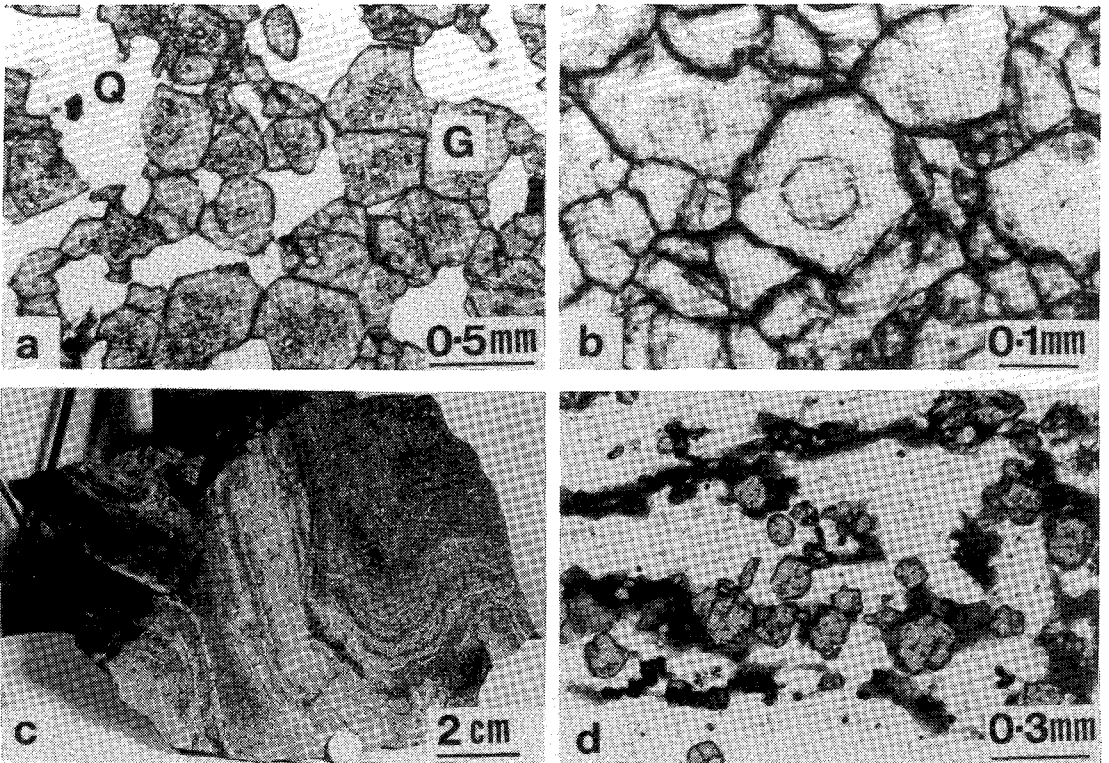


FIG. 4. a. Garnet (G) with quartz inclusions in quartz garnetite. The white mineral is quartz (Q), plane-polarized light. b. Garnet overgrowth on pre-existing garnet in garnetite, plane-polarized light. c. Folded sample of garnetite showing alternating layers of garnet (light-colored bands) and sphalerite-galena intergrowths (dark-colored bands). d. Banding produced by biotite and garnet in quartz-biotite garnetite, plane-polarized light.

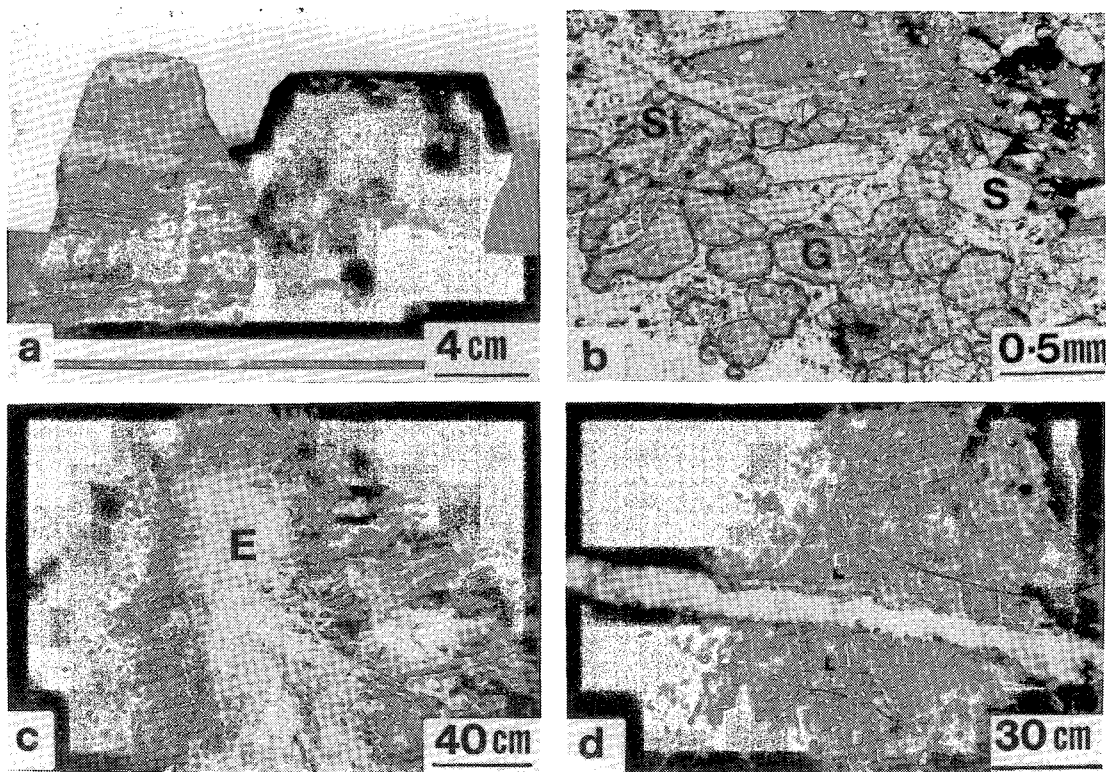


FIG. 5. a. Banded quartz garnetite (left) and sulfide-bearing banded iron-formation (right). b. Intergrowth of staurolite (St), sillimanite (S), garnet and biotite in sillimanite-quartz garnetite, plane-polarized light. c. Garnet envelope (E) on the margin of the 2 lens orebody. Note the rows of garnet parallel to a schistosity in the wallrocks that formed during a retrograde metamorphic event. d. Garnet envelope surrounding a quartz vein in quartz garnetite.

(Fig. 5c). A second type of garnet envelope, previously undescribed, occurs around late-stage quartz-fluorite veins in 2 lens (N.B.H.C. mine) and quartz veins in Zinc lode at N.B.H. mine (Fig. 5d).

CHEMISTRY OF GARNET-RICH ROCKS

Major elements

Compositions of 17 samples of quartz-bearing garnetite (predominantly quartz-garnetite) are shown in Figure 6a, and representative compositions are shown in Table 3. MgO was omitted from Figure 6a and 6b because it is generally less than 1%. Despite the small number of analyses and the predominance of quartz-garnetite, it is apparent that quartz-bearing garnetites from 2 lens contain a high proportion of Ca and Fe, those from 3 lens, a high proportion of Mn, and those from B lode and 1 lens, a high proportion of Fe. Additional compositions of

some quartz-bearing garnetites from the southern mines are reported in Billington (1979).

Results of analyses of 16 samples of garnetite were reported by the Geological Subcommittee (1910), Andrews (1922), Stillwell (1922, 1959) and McKay (1974). McKay (1974) analyzed two samples adjacent to the 2 lens (N.B.H.C. mine), and Stillwell (1959) indicated that one sample was collected adjacent to the 3 lens at Broken Hill South (B.H.S.) mine. The other 13 samples came from the B.H.S. mine, but there is no record of the nature of the orebody associated with these samples. Despite this, Black (1953), in his description of the geology of B.H.S. mine, indicated that garnetite is confined to the 3 lens. Results of one new analysis of garnetite rock from the 3 lens (Z.C. mine, anal. 11, Table 3) are plotted with the previous 16 analyses of garnetite in Figure 6b.

The only analyzed sample of garnet envelope that surrounds a quartz vein from the Zinc lode (N.B.H. mine) contains 7.6% MnO and 0.8% CaO (anal. 12, Table 3). Billington (1976) reported approximately

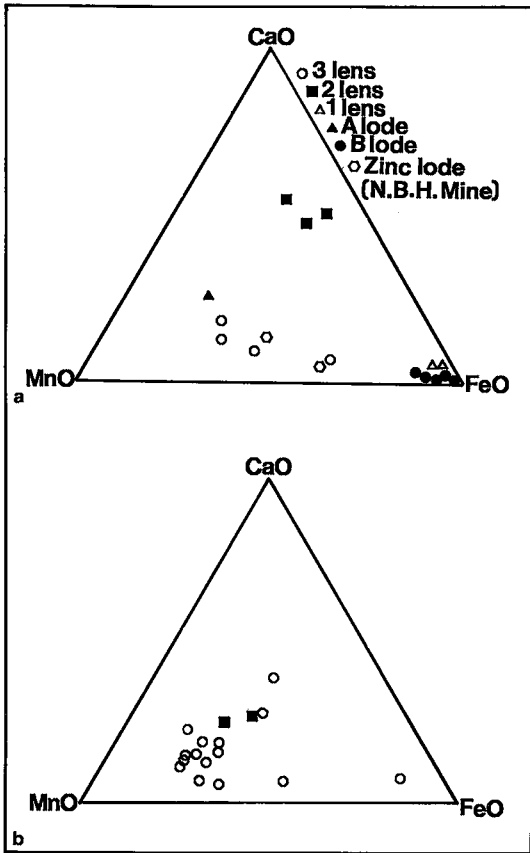


FIG. 6. a. Triangular CaO-MnO-FeO plot showing compositions of quartz-bearing garnetite. b. Triangular plot showing garnetite compositions; data for 2 lens samples are from McKay (1974). All but two of the open circles represent data from Black (1953), which are likely for garnetites from the 3 lens (B.H.S.). The other two data points are samples from 3 lens (Stillwell 1959, this study).

10% CaO and 10% MnO in two samples of garnet envelope adjacent to the 2 lens (N.B.H.C. mine).

Composition of garnet

Previous studies of the composition of garnet within or in close proximity to the Broken Hill lode include those of Hodgson (1975), Stanton (1976), Stanton & Williams (1978) and Plimer (1976, 1979). Hodgson (1975) examined the compositional relationship between garnet and coexisting pyroxenoid minerals in the lode, and Stanton (1976) analyzed the garnet in a transect across the B lode. In a 1000-m section enclosing the Broken Hill deposit, garnet in pelitic, psammitic and quartzofeldspathic rocks was shown by Plimer (1976, 1979) to be Fe-rich.

Quartz-bearing garnetite and garnetite constitute approximately 95% of the garnet-rich rocks associated with the Broken Hill deposit. Since they consist of garnet and quartz mainly, the variation in the composition of garnet will be an excellent indicator of the variation of Mn, Fe, Ca, Mg, and Al in these rocks.

Garnet in 21 samples of quartz-bearing garnetite, 7 of garnetite, and 3 of garnet envelope was analyzed using an Etec Autoprobe at the University of Sydney. Operating conditions, using wavelength dispersion, were: accelerating voltage of 14.2 kV and a specimen current of between 0.04 and 0.07 μ A. Garnet (Mg, Al, Fe, and Si), rhodonite (Mn), wollastonite (Ca) and rutile (Ti) were used as standards. The electron microprobe was connected to an Interdata computer system providing on-line data reduction. The operating programs are written in BASIC, and data correction is based on a ZAF-type program. Electron-microprobe data were corrected for dead-time, background and beam-current-monitored drift prior to ZAF correction. The garnet compositions are presented in Figures 7a and b, and representative compositions are shown in Table 4.

Garnet in quartz-bearing garnetite from B and C lodes is almandine-rich (anal. 8, 9, 10, Table 4), and similar in composition to garnet analyzed by Plimer (1976) from country-rock gneisses and schists surrounding the deposit. However, garnet in garnet-rich rocks from other lenses contains lower proportions of the almandine component. Orange or brown garnet from the 3 lens and A lode quartz-bearing garnetites and garnetites generally contains a high proportion of spessartine (anal. 1, 2, 6, 7, Table 4), whereas garnet from the same type of rock in the 2 lens is rich in the grossular component (anal. 4, 5, Table 4). Although pink garnet is rare within the Lead lodes, it is rich in the almandine component (anal. 3, Table 4).

Garnet in garnet envelope is optically and compositionally zoned (Fig. 8). Small inclusions of quartz typically separate overgrowths of garnet on earlier-formed cores. Overgrowths are generally depleted in almandine and pyrope and rich in spessartine and grossular relative to the cores (anal. 12, Table 4), regardless of the mineral in contact with it. In contrast, garnet in quartz-bearing garnetite and garnetite is generally homogeneous in composition (anal. 11, Table 4). Exceptions exist where these rocks are spatially associated with garnet envelope, late-stage quartz veins, and shear zones.

DISCUSSION

Origin of the garnet-rich rocks

Hodgson (1975) and Lee (1977) suggested that

TABLE 3. BULK-ROCK CHEMICAL DATA OF GARNET-RICH ROCKS*

Sample No.	1 3	2 284	3 303	4 343	5 219A	6 231	7 241	8 46	9 107	10 319	11 120	12 315
SiO ₂ %	76.86	56.35	65.32	57.84	69.65	63.95	56.70	48.97	40.30	75.71	36.82	55.75
TiO ₂	0.33	0.14	0.30	0.43	0.71	0.52	0.05	0.48	0.44	0.75	0.57	0.67
Al ₂ O ₃	6.57	13.77	9.81	12.60	12.02	11.45	12.16	15.18	18.26	11.26	18.99	17.16
Fe ₂ O ₃ **	9.98	8.47	18.75	23.38	13.71	8.10	7.17	14.39	12.67	5.42	10.17	14.74
MnO	1.38	16.02	1.30	1.48	0.80	3.69	5.22	16.80	22.58	3.02	25.19	7.57
MgO	1.70	0.16	1.74	2.59	1.32	0.19	0.13	0.54	0.57	0.40	0.23	0.86
CaO	0.15	5.61	1.04	0.32	0.21	10.77	14.94	3.17	5.29	0.46	6.19	0.79
Na ₂ O	0.23	0.02	0.07	0.02	0.14	0.06	0.03	0.03	0.07	0.09	0.04	0.14
K ₂ O	1.67	0.00	0.99	0.60	1.20	0.77	0.12	0.03	0.17	2.47	0.00	2.68
P ₂ O ₅	0.02	0.02	0.05	0.06	0.03	0.05	2.31	0.16	0.07	0.05	0.11	0.05
SO ₃	0.02	0.00	0.00	0.01	0.00	0.00	0.00	0.00	0.00	0.00	0.02	0.00
Cu	0.05	0.00	0.00	0.03	0.01	0.00	0.00	0.04	0.00	0.00	0.17	0.00
Pb	0.07	0.07	0.02	0.03	0.01	0.00	0.79	0.10	0.01	0.00	1.40	0.01
Zn	0.06	0.00	0.28	0.02	0.00	0.10	0.01	0.14	0.01	0.00	0.05	0.00
Loss**	0.09	0.00	0.17	0.00	0.15	0.16	0.03	0.00	0.00	0.20	0.01	0.02
	99.48	100.63	99.84	99.41	99.96	99.81	99.66	100.03	100.44	99.83	99.96	100.44

*Total Fe expressed as Fe₂O₃; **Fusion loss; 1. quartz garnetite, B lode (N.B.H.C. mine); 2. quartz garnetite, A lode (N.B.H.C. mine); 3. quartz garnetite, 1 lens (Z.C. mine); 4. quartz garnetite, 1 lens (N.B.H.C. mine); 5. sillimanite-quartz garnetite, B lode (N.B.H.C. mine); 6. quartz garnetite, 2 lens (N.B.H. mine); 7. quartz garnetite, 2 lens (N.B.H. mine); 8. quartz garnetite, 3 lens (N.B.H. mine); 9. quartz garnetite, 3 lens (N.B.H. mine); 10. quartz garnetite, Zinc lode (N.B.H. mine); 11. quartz garnetite, 3 lens (Z.C. mine); 12. garnet envelope, Zinc lode (N.B.H. mine). *MnO analyses determined by flame photometry, Cu-Zn-Pb analyses determined by Techron AA-6 absorption spectrophotometer, sulfur analyses by Leco Automatic Sulfur Determinator, all other oxides determined by X-ray fluorescence techniques using a Siemens SRS machine (University of Adelaide).

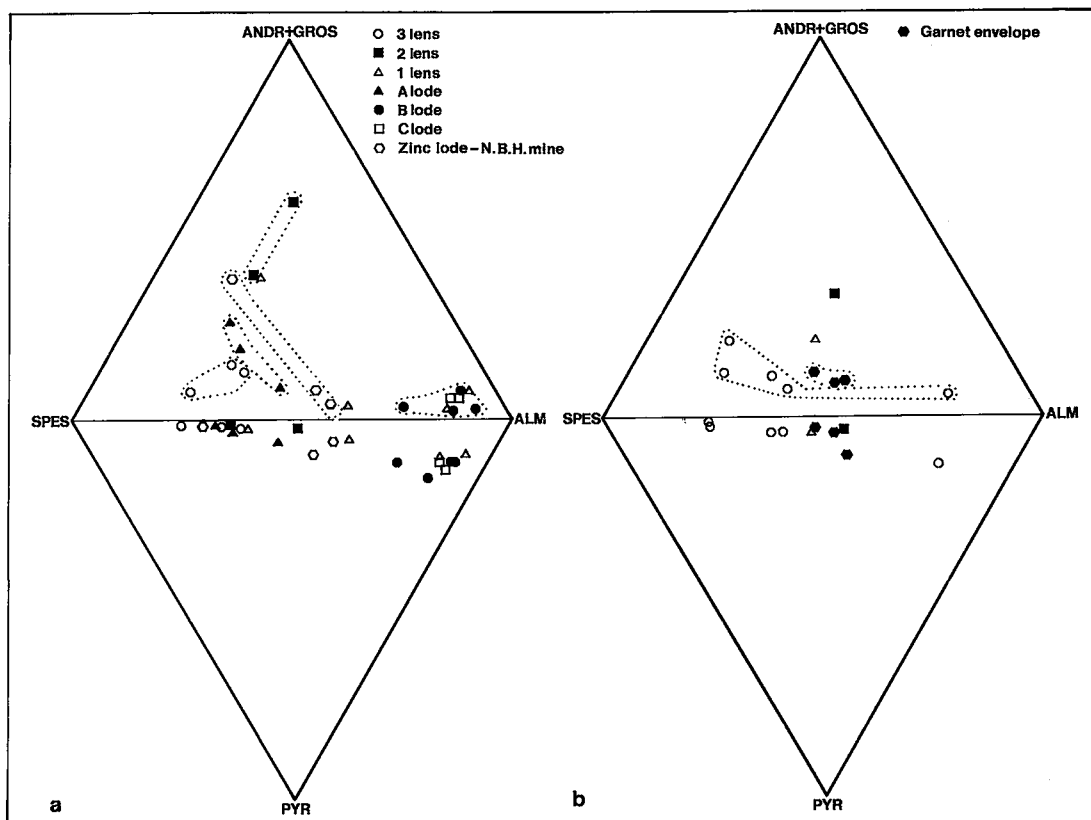


FIG. 7. a. Composition of garnet in quartz-bearing garnetite in terms of almandine (ALM), spessartine (SPES), pyrope (PYR), and andradite + grossular (ANDR + GROS). Areas outlined by dots enclose garnet compositions from the same orebody. b. Composition of garnet in garnetite and garnet envelope.

TABLE 4. CHEMICAL COMPOSITIONS OF GARNET IN GARNET-RICH ROCKS

Sample No.	1		2		3		4		5		6		7		8		9		10		11		12	
	center	edge	center	edge																				
SiO ₂	36.97	36.76	37.54	37.82	38.07	38.15	36.24	37.06	37.01	37.34	37.03	36.76	38.20	18.76										
TiO ₂	0.09	0.10	0.02	0.18	0.10	0.00	0.11	0.04	0.00	0.01	0.05	0.01	0.00	0.00							0.01	0.00	0.00	
Al ₂ O ₃	19.75	20.30	20.88	20.54	20.79	18.19	21.04	21.11	21.45	21.61	21.29	21.35	20.49	20.34							21.35	20.49	20.34	
Fe ₂ O ₃ *	1.18	0.79	0.19	0.93	1.25	3.70	0.00	0.00	0.00	0.00	0.00	0.00	0.65	0.81						0.00	0.65	0.81		
FeO	10.19	8.42	29.38	16.61	9.98	11.27	11.06	33.91	31.52	32.73	23.13	23.16	22.89	17.74						23.16	22.89	17.74		
MnO	29.71	26.79	7.23	12.77	9.07	21.57	22.63	3.38	4.86	4.23	15.74	15.90	15.77	17.29						15.90	15.77	17.29		
MgO	0.16	0.28	2.92	0.18	0.17	0.70	0.30	2.78	4.44	3.39	1.94	1.75	1.72	0.88						1.75	1.72	0.88		
CaO	2.61	6.31	1.58	11.31	20.58	6.27	8.69	1.95	0.91	0.70	0.92	0.95	0.76	4.07						0.95	0.76	4.07		
TOTAL:	100.66	99.75	99.74	100.34	100.11	99.85	100.07	100.34	100.23	100.01	100.10	99.88	100.48	99.89										
Atomic Proportions (cation basis 16)																								
Si	6.016	5.984	6.067	6.058	5.964	6.221	5.842	5.966	5.900	6.003	6.057	5.979	6.189	6.294										
Ti	0.012	0.012	0.012	0.002	0.012	0.000	0.014	0.004	0.000	0.002	0.006	0.002	0.000	0.000							0.002	0.000	0.000	
Al ³⁺	3.840	3.893	3.975	3.876	3.837	3.495	4.000	4.006	4.031	4.093	4.104	4.093	3.912	3.890							4.093	3.912	3.890	
Fe ³⁺	0.160	0.107	0.025	0.124	0.163	0.505	0.000	0.000	0.000	0.000	0.000	0.000	0.088	0.110						0.000	0.088	0.110		
Fe ²⁺	1.386	1.145	3.743	2.224	1.304	1.536	1.491	4.563	4.200	4.397	3.163	3.148	3.101	2.407							3.148	3.101	2.407	
Mn	4.094	3.693	0.989	1.732	1.203	2.978	3.087	0.460	0.656	0.575	2.180	2.191	2.163	2.378							2.191	2.163	2.378	
Mg	0.038	0.066	0.704	0.042	0.062	0.172	0.072	0.666	1.057	0.810	0.473	0.423	0.415	0.212							0.423	0.415	0.212	
Ca	0.454	1.101	0.273	1.940	3.453	1.094	1.499	0.336	0.156	0.120	0.016	0.166	0.137	0.709							0.166	0.137	0.709	
Garnet Proportions																								
Almandine	23.21	19.06	64.66	37.45	21.65	23.49	24.25	75.94	69.39	73.16	52.58	52.68	52.14	42.18										
Andradite	4.15	2.68	0.86	3.13	4.07	13.11	0.00	0.00	0.00	0.00	0.00	0.00	2.21	2.89							0.00	2.21	2.89	
Grossular	3.58	15.67	3.85	29.54	53.28	5.81	24.38	5.37	2.35	4.27	4.24	4.71	2.30	9.53							4.71	2.30	9.53	
Pyrope	0.63	1.11	13.54	0.71	1.03	2.98	1.17	11.04	17.42	13.19	7.68	6.88	6.98	3.72							6.88	6.98	3.72	
Spessartine	68.55	61.49	17.08	29.17	19.97	51.52	50.20	7.65	10.83	9.38	35.39	35.66	36.37	41.68										

*Fe₂O₃ calculated from the Fe³⁺ content, the latter was determined from Al³⁺ deficiencies in the octahedral site; 1. quartz garnetite (orange-colored garnet), 3 lens (N.B.H. mine); 2. garnetite (orange-colored garnet), 3 lens (N.B.H. mine); 3. garnetite (pink-colored garnet), 3 lens (N.B.H. mine); 4. garnetite (orange-colored garnet), 2 lens (N.B.H.C. mine); 5. quartz garnetite (orange-colored garnet), 2 lens (N.B.H.C. mine); 6. quartz garnetite (orange-colored garnet), A lode (N.B.H.C. mine); 7. quartz garnetite (orange-colored garnet), A lode (N.B.H.C. mine); 8. quartz garnetite (red-colored garnet), B lode (Z.C. mine); 9. quartz-garnetite (red-colored garnet), B lode (N.B.H.C. mine); 10. quartz-garnetite (red-colored garnet), C lode (Z.C. mine); 11. quartz garnetite (brown-colored garnet); Zinc lode (N.B.H. mine); 12. garnet envelope (orange-brown colored garnet), Zinc lode (N.B.H. mine).

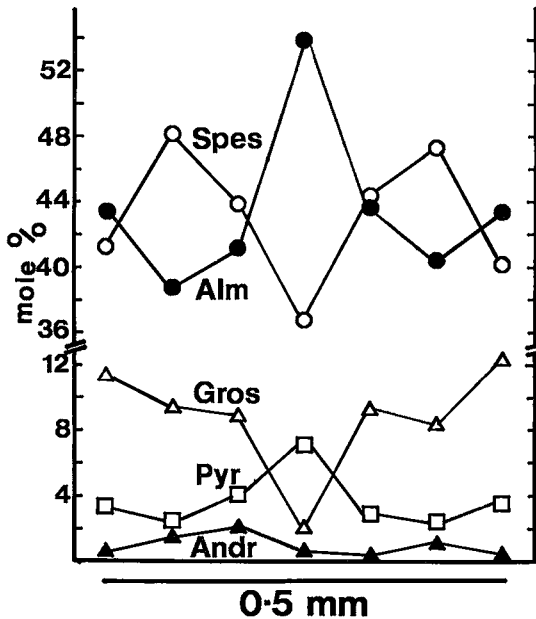


FIG. 8. Compositional profile across garnet in garnet envelope, sample 318, Zinc lode, N.B.H. mine. Symbols: ALM almandine, ANDR andradite, GROS grossular, PYR pyrope, and SPES spessartine.

quartz-bearing garnetite and garnetite at Broken Hill were derived by Mn-Ca-rich fluids that were sweated out of the Mn-Ca-bearing orebodies and that reacted with the Al-rich wall-rocks during a prograde metamorphic event. The inference, therefore, is that these garnet-rich rocks should have formed only where economic Pb-Zn-Ag mineralization was present. Such a suggestion is untenable because these rocks occur without Pb-Zn-Ag throughout the Willyama Complex.

Suggested precursors to the garnet-rich rocks are manganese chamositic beds (Stanton 1976) and variants of original clean detrital sands (Haydon & McConachy 1987). Stanton considered that pennantite (a manganese thuringite) has a suitable composition to be a precursor of spessartine garnet. Although chlorites such as pennantite and thuringite could produce the variations in Mn, Fe, and Mg content in garnet, there is no apparent way by which these or any other chlorites could give rise to the grossular or andradite component of garnet in garnetite or quartz-bearing garnetite. A Ca-bearing mineral such as calcite or plagioclase would have to be incorporated into the chlorite-rich sediments. The main problem with Stanton's (1976) suggestion relates to the amount of pennantite that would be required to produce the large volume of garnet-rich rock in the Broken Hill lode and throughout the

Willyama Complex. Pennantite is a rare chlorite in nature and has not been reported in the amounts necessary to form the extensive Mn-bearing horizons at Broken Hill. Similarly, unmetamorphosed equivalents of extensive manganese-bearing "clean detrital sand units" as envisaged by Haydon & McConachy (1987) also are unknown.

Possible models to account for manganeseiferous sediments on the seafloor include halmyrolysis of basalt, low-temperature precipitation as nodules and crusts, with diagenetic enrichment in the sediment column, and formation from hydrothermal vents (*e.g.*, Wonder *et al.* 1988). A recent model proposed by Huebner *et al.* (1986) to account for the manganese-rich metasediments in the Buckeye mine, California, envisages Mn-gel forming at the sediment-seawater interface and reacting with biogenic silica. Although each of these models may account for the high Mn and Si content of the garnet-rich rocks at Broken Hill, all are unable to account for the high Al content of many of the garnetites and quartz-bearing garnetites.

Trace elements such as Cu, Co and Ni are known to be more concentrated in hydrogenous Fe-Mn sediments than in hydrothermal sediments, largely because of the accumulation rate of hydrogenous sediment is much slower than for hydrothermal sediments, allowing scavenging of these seawater-derived elements by Fe- and Mn-mineral particles (Bonatti *et al.* 1972, Toth 1980). Data for Cu, Co, Ni, Fe and Mn reported by Billington (1979) and recent rare-earth-element analyses by Plimer & Lottermoser (1988) of garnet-rich rocks from the Broken Hill deposit show that they have a chemical signature characteristic of hydrothermal sediments from the Red Sea and the East Pacific Rise.

The most plausible model to explain the presence of garnetite and quartz-bearing garnetite at Broken Hill is for them to have formed near hydrothermal vents on the ocean floor. Likely precursors to garnet in garnet-rich rocks are minerals such as manganite, pyrolusite, hausmannite, vernadite or pyrochroite; these phases commonly are observed near hydrothermal vents on the ocean floor (*e.g.*, Dymond *et al.* 1973, Hackett & Bischoff 1973). Not only could this type of setting account for the continuity of the manganeseiferous rocks, but Fe minerals such as hematite and goethite also are spatially related. Boström & Peterson (1969) have described manganese- and iron-rich oxides in calcium carbonates on the ocean floor. If these minerals were incorporated with detrital Al-Mg-bearing clays, all the requisite elements would be present to account for those present in garnet and most other minerals observed in quartz-bearing garnetites and garnetites.

Billington (1976) suggested that the precursor to garnetite originated by the introduction of Mn into unconsolidated pelitic sediments beneath the basin

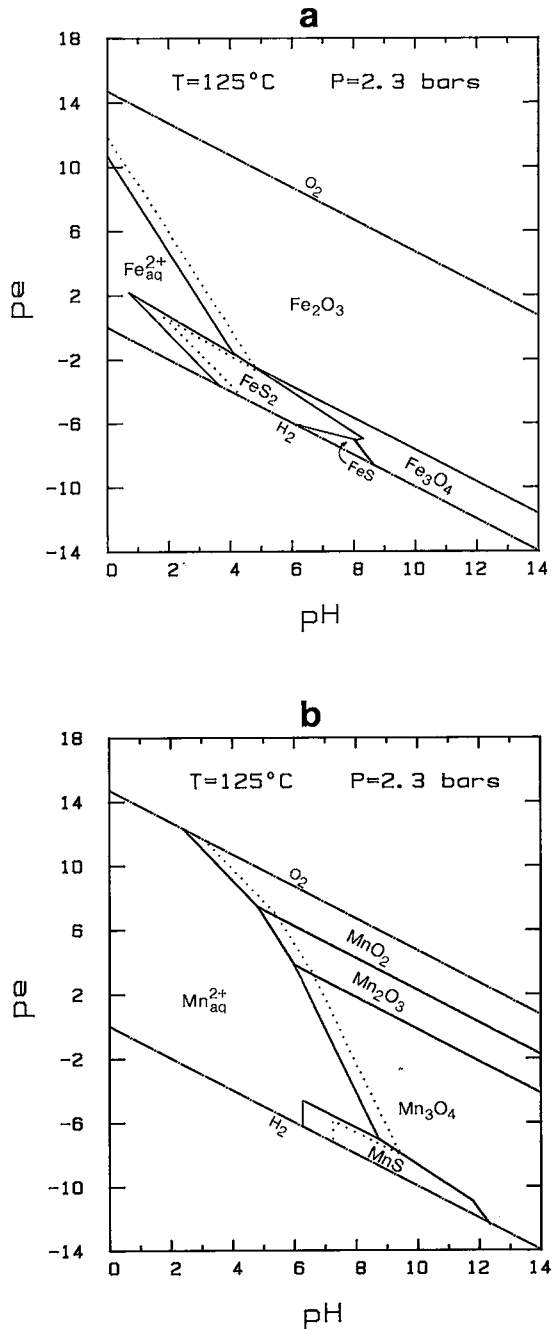


FIG. 9. Mineral-solution stability diagrams with respect to pe and pH at $125^{\circ}C$, 2.3 bars, total aqueous sulfur activity of 0.01, and aqueous metal species activities of 10^{-5} (solid lines) and 10^{-6} (dotted contour). a. Stability fields for aqueous Fe and Fe oxides and sulfides. b. Stability fields for aqueous Mn and Mn oxides and sulfide.

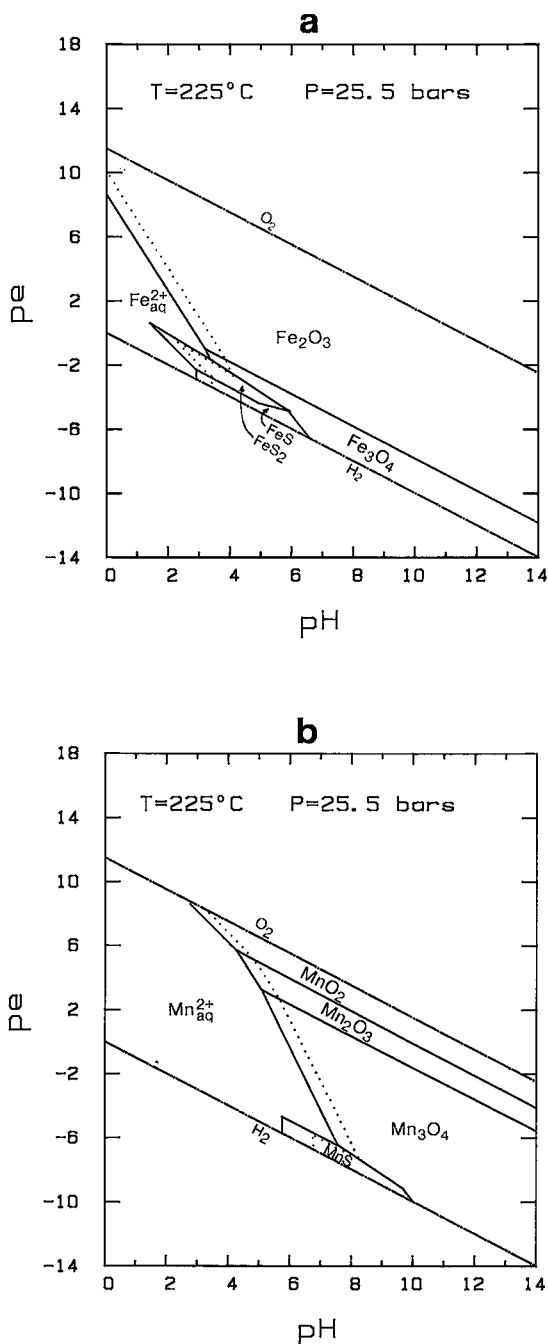


FIG. 10. Mineral-solution stability diagrams with respect to pe and pH at 225°C , 25.5 bars, total aqueous sulfur activity of 0.01 , and aqueous metal species activities of 10^{-5} (solid lines) and 10^{-6} (dotted contour). a. Stability fields for aqueous Fe and Fe oxides and sulfides. b. Stability fields for aqueous Mn and Mn oxides and sulfide.

of sulfide deposition. Billington's model, however, does not account for garnetite on both margins of the 3 lens at N.B.H. mine, not just on the footwall side. Billington (1976) also suggested that garnet envelope was formed during the prograde metamorphic event, whereas Maiden (1972) considered that the envelope was formed during both the prograde and retrograde metamorphic events. Because garnet in garnet envelope forms trains that are parallel to retrograde schistosity or that cut across schistosity formed during a prograde metamorphic event, it is suggested that garnet envelope was formed by the metasomatic replacement of Al-rich wallrocks by Mn and Ca during a retrograde metamorphic event. This suggestion is supported by the spatial association of garnet envelope with late-stage quartz-fluorite veins (W.P. Laing, oral comm. 1978), the incorporation of late marcasite, pyrite and monoclinic pyrrhotite in the garnet halo, and the pattern of compositional zonation in garnet. In quartz-bearing garnetite and garnetite, garnet is typically homogeneous in composition, as is garnet metamorphosed to granulite grades elsewhere (e.g., Tracy 1982). However, garnet in garnet envelope commonly shows an overgrowth enriched in spessartine and grossular and depleted in pyrope and almandine, and a garnet core that has the composition of garnet in quartz-bearing garnetite across which the garnet envelope cuts. The garnet core is interpreted to have formed during a prograde metamorphic event, whereas the overgrowth formed during a retrograde metamorphic event.

Chemical relationship of Mn and Fe at the Broken Hill deposit

If we assume a hydrothermal source for the ore-bearing components, including Mn and Fe, and a vent-type setting on the ocean floor, we must be able to explain the increase in the ratio Mn/Fe from the footwall to the hanging wall of the Broken Hill deposit under the physicochemical conditions likely to be encountered at an ore-forming hydrothermal vent.

Experimental studies by Bischoff & Dickson (1975), Seyfried & Bischoff (1977), and Mottl *et al.* (1979) have shown that heavy metals, including Mn and Fe, can be transported in significant quantities by circulation of seawater through hot oceanic basalt. Furthermore, these studies have shown that the relative abundance of Fe and Mn in solution depends on parameters such as pH , T , the water-to-rock ratio, and the degree of solution-to-rock equilibration.

The stabilities of phases of the system Mn-Fe-O-H in Eh - pH space at 25°C were calculated by Crerar *et al.* (1980). However, the stability of the system has

not been calculated at the temperatures (100–350°C) that are likely to be encountered in the formation of massive sulfide deposits. It is unknown whether the same topology determined by Crerar *et al.* (1980) at 25°C is maintained in the system Mn–Fe–O–H at higher temperatures.

Redox equilibria were calculated for Fe and Mn oxide and sulfide species at 125° and 225°C and pressures corresponding to the H₂O liquid–vapor saturation curves using equations and data from Helgeson & Kirkham (1974), Robie *et al.* (1978), and Helgeson *et al.* (1981) (Figs. 9a, b, 10a, b). The boundaries between aqueous ions and oxide and sulfide species of Fe and Mn shift to slightly lower values of *pH* and *pe* with increasing temperature. The Fe boundaries remain at significantly lower *pe* conditions than the Mn boundaries at 125° and 225°C; however, boundaries for the Mn species shift slightly more than the boundaries for the Fe species in *pe*–*pH* space at these temperatures.

Although simple aqueous ions may be the dominant species in lower-temperature solutions (*i.e.*, 25 – 225°C), chloride complexes are the dominant aqueous species for Fe (Boctor *et al.* 1980) and Mn (Boctor & Frantz 1980) at temperatures of 400 – 700°C. Therefore, oxidation boundaries for FeCl₂ and MnCl₂ were determined at 325°C (Figs. 11a, b) by extrapolating higher-temperature data from Boctor *et al.* (1980), Frantz & Marshall (1984) and Boctor (1985). Oxidation of MnCl₂ to Mn oxides occurs at lower *pH* and *pe* values than those for Mn²⁺ ions (Fig. 12a), but oxidation of FeCl₂ occurs at higher *pe* and *pH* than does Fe²⁺ ion. In summary, the Fe minerals are stable to less oxidizing conditions than corresponding Mn minerals at all temperatures, and for both simple ions and chloride complexes, given equal concentrations in solution.

Also imparting an influence on the location of the oxidation boundaries is the concentration (activity) of metal in solution. The heavy lines in Figures 9a to 10b represent activities of 10⁻⁵. The boundaries occur at higher *pH* and *pe* values for lower activities (dotted contours). The sulfide fields are dependent on metal activity and activity of aqueous sulfur species.

To determine how these phase diagrams apply to a seafloor hydrothermal environment, a mixing path between an exhaling hydrothermal solution and ambient seawater must be approximated. Seawater is slightly alkaline (*pH* ranging from 7.5 to 8.0) and oxidizing. Uncontaminated hydrothermal fluids are acidic (*pH* between 3 and 5) and reducing. The hydrothermal fluid is based on East Pacific Rise (EPR) fluid (Bowers *et al.* 1985). The hydrothermal fluid's *pe* value is restricted by the position of the equilibrium boundaries of the aqueous sulfur species, as H₂S is the dominant sulfur species in these fluids (*cf.* Seyfried & Bischoff 1977). The mixing

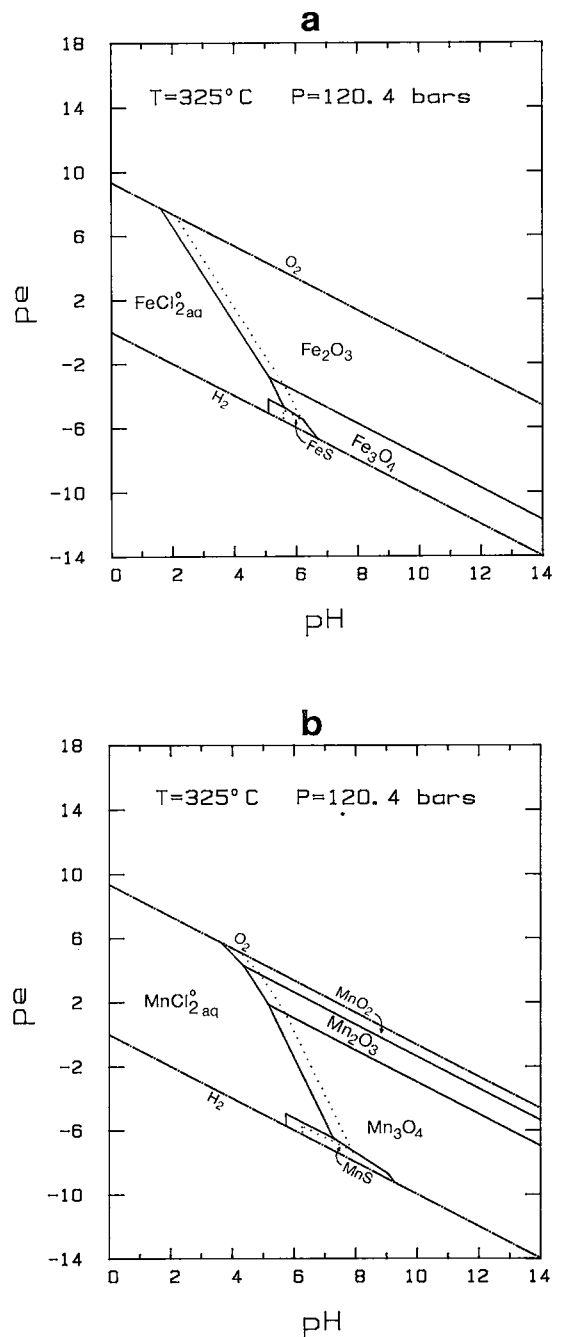


FIG. 11. Mineral–solution stability diagrams with respect to *pe* and *pH* at 325°C, 120.4 bars, total aqueous sulfur activity of 0.01, aqueous chlorine activity of 0.35, and aqueous metal activities of 10⁻⁵ (solid lines) and 10⁻⁶ (dotted contour). a. Stability fields for aqueous FeCl₂ and Fe oxides and sulfides. b. Stability fields for MnCl₂ and Mn oxides and sulfide.

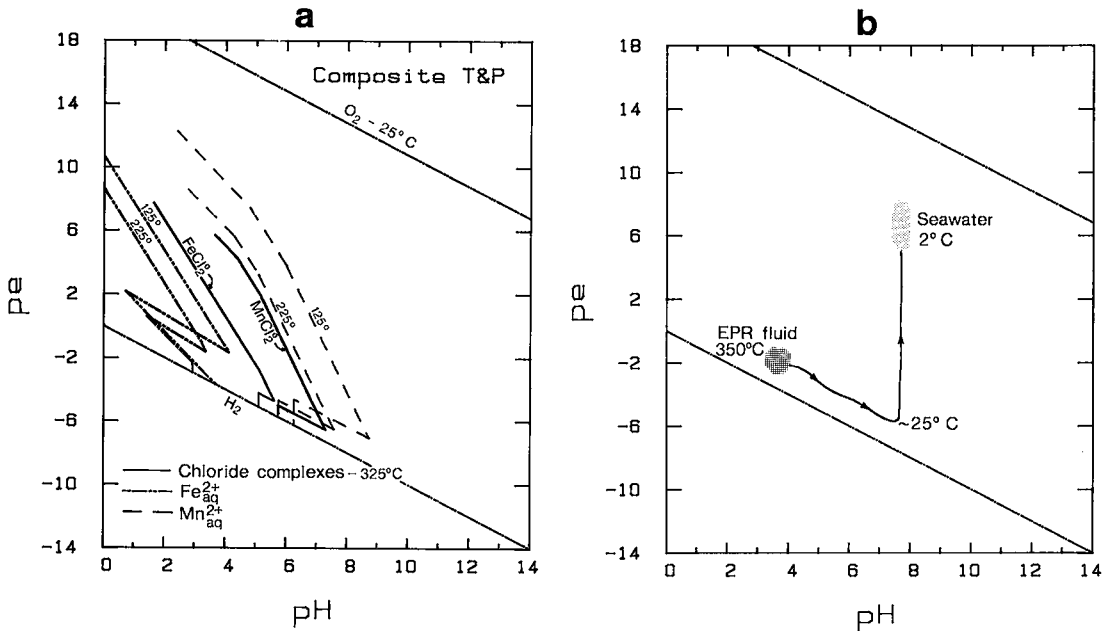


FIG. 12. a. Composite of solution–mineral boundaries for simple aqueous Fe and Mn cations at 125° and 225° and for aqueous chloride complexes at 325° . b. Theoretical mixing path between East Pacific Rise (EPR) hydrothermal fluid and seawater (after Bowers *et al.* 1985).

path for these two fluids can be inferred from theoretical work of Bowers *et al.* (1985). They modeled the evolution of hydrothermal fluids due to conductive cooling within a sediment pile and by energetic mixing with ambient seawater. With the addition of seawater, the temperature of the combined solution drops linearly with respect to the extent of mixing from an initial value of about $350^\circ C$. Similarly, the $f(O_2)$ (analogous to p_e) decreases, and pH increases. These changes continue until the solution exceeds approximately 90% seawater, whereupon $f(O_2)$ of the solution increases rapidly in response to seawater domination of the system. This theoretical mixing is qualitatively represented in Figure 12b.

Comparison of Figures 12a and 12b reveals that the EPR fluid field lies entirely within the oxide + sulfide field at temperatures relevant to the chloride-free system but falls on the solution side of the $FeCl_2$ boundary. The simple ion is probably not the dominant species in solution at temperatures near that of the EPR fluid, but as it becomes dominant at lower temperatures, the precipitation of Fe sulfides (and oxides?) along the mixing path may partly be the result of the change in the character of the dominant aqueous species. The EPR fluid region lies on the solution side of all the Mn boundaries, and it is clear from Figure 12 that $MnCl_2$ is probably not

responsible for any Mn mineral precipitation. Mn oxide– Mn^{2+} boundaries are not reached until the last 20–30% of the drop in temperature (*i.e.*, the last 6–9% of mixing).

One shortcoming inherent in this analysis is that complexation behavior of Fe and Mn in aqueous solutions has not been investigated experimentally at temperatures between $25^\circ C$ and 400 – $700^\circ C$ (at which chloride complexes are known to predominate). The calculations for $325^\circ C$ assume that chloride complexes remain dominant at low temperature; the transition from chloride-complex dominance to aqueous-cation dominance is not understood, yet this knowledge is necessary for a full understanding of the processes.

Compounding the temporal separation of Fe and Mn precipitation from a hydrothermal fluid – seawater mixture are the extremely slow kinetics of Mn^{2+} oxidation (Morgan 1967). Manganese ions will not precipitate as oxides immediately upon entrance into the oxide stability fields but may remain in solution for a considerable time and thus be carried for a substantial distance before precipitation occurs. If Mn were sufficiently more concentrated in solution than Fe, Mn oxides or sulfide might be precipitated before Fe oxides or sulfides, depending ultimately upon kinetics.

Spatial variations in the ratio Fe/Mn in naturally

occurring deposits, such as near oceanic spreading centers (e.g., Scott *et al.* 1974, Corliss *et al.* 1978) and in ancient massive sulfide deposits (e.g., Vaughan & Stanton 1986), have been commonly observed. The work of Hawkins (1968) and Plimer (1979) suggests that there is a general increase in Mn/Fe from the footwall to the hanging wall of the Broken Hill deposit and along strike from south to north. However, it should be pointed out that Stanton *et al.* (1978) have shown that the Mn content does not increase systematically from footwall to hanging wall because the B lode and 1 lens are generally deficient in Mn, whereas the A lode and 3 lens are rich in Mn. The Mn content of the 2 lens is intermediate between these two groups and is, by contrast, rich in Ca. The compositions of the garnet-rich rocks and the contained garnet reflect the same compositional variations exhibited by the orebodies.

Because of the effects of granulite-grade metamorphism on the Broken Hill deposit, the original ore-forming conditions are unknown. However, the calculations involving Mn and Fe suggest that temperature does not drastically affect the topology or position of the equilibrium fields of Mn and Fe-bearing phases. The Fe content of the orebodies and the enclosing country rocks is constant; consequently, there is no reason to suggest that the Fe content of the ore-forming solution at Broken Hill varied considerably during ore deposition. Therefore, the most likely cause for the fluctuation in the ratio Mn/Fe across the Broken Hill deposit is the variation in Mn concentration in the ore-forming solution during ore deposition. The overall increase in Mn/Fe reflects an increase in $f(\text{O}_2)$ during deposition that resulted when the ore-forming fluid mixed with seawater.

There are two important features of the proposed suggestions: they help to explain the presence of the most Mn-rich garnet rock on the stratigraphic hanging wall of the 3 lens, and the variation in Mn/Fe across sulfide deposits may occur at a variety of temperatures.

Manganoan garnet-rich rocks as a guide to exploration

Like iron formations and tourmalinites, Mn anomalies have been recognized as guides in the exploration for massive sulfide deposits (e.g., Wonder *et al.* 1988). These Mn anomalies may be recognized as manganiferous limestone beds (e.g., Tynagh: Russell 1974), rhodocrosite in sulfides (e.g., Rosebery: Braithwaite 1974), unmetamorphosed ferromanganiferous sediments associated with mid-ocean ridges (e.g., Scott *et al.* 1974), or garnet-bearing rocks (e.g., Gamsberg: Stumpf 1979). Although the presence of Mn garnet has been suggested as a guide to mineralization (e.g., Valliant & Barnett

1982), and have been used as a guide to ore in the Willyama Complex for years, the garnet-bearing rocks themselves have received minimal attention. In addition to simple garnet-quartz rocks, or coticles, garnet-bearing rocks should be carefully considered as exploration guides. It is clear from the present study that at least six varieties of quartz-bearing garnetite, in addition to quartz garnetite, or coticule, are associated with mineralization at Broken Hill. Some of these varieties of garnetite have been recognized in association with other sulfide occurrences. Key areas where the use of garnet-bearing rocks warrant particular attention are the Mt. Painter Block in South Australia, the Namaqualand Province, South Africa, and the Appalachians, United States.

ACKNOWLEDGEMENTS

We thank R.A. Both for his suggestions and invaluable discussions, and acknowledge the cooperation and many discussions with mine personnel at Broken Hill, without whose help this project would not have been possible. K.L. Williams and K. Moran from the University of Sydney are thanked for their assistance with access to the electron microprobe. This manuscript was improved considerably by the reviews of J.L. Jambor, J.S. Huebner, and M.L. Williams. Funding of this project was provided by the Broken Hill Mine Managers' Association and an Australian Postgraduate Research Award to P.G.S., and by the Iowa State Mining and Mineral Resources Research Institute through the Department of the Interior's Mineral Institutes program, administered by the U.S. Bureau of Mines under Allotment Grants G1144119, G1154119, and G1164119.

REFERENCES

- ANDREWS, E.C. (1922): The geology of the Broken Hill district. *Geol. Surv. New South Wales Mem.* 8.
- BARNES, R.G., STEVENS, B.P.J., STROUD, W.J., BROWN, R.E., WILLIS, I.L. & BRADLEY, G.M. (1983): Zinc, manganese, and iron-rich rocks and various minor rock types. *Geol. Surv. New South Wales Records* 21, 289-323.
- BILLINGTON, L.G. (1976): *Geochemistry and Origin of Garnet-Rich Rocks Around the Lead Lode, N.B.H.C. Mine, Broken Hill, N.S.W.* Preliminary M.S. thesis, Univ. New South Wales, Broken Hill, Australia.
- ____ (1979): *The Relationship of the Garnet Quartzite Rock Types to the Orebodies in the ZC-NBHC mines, N.S.W., Australia.* M.S. thesis, Univ. New South Wales, Broken Hill, Australia.

- BISCHOFF, J.L. & DICKSON, F.W. (1975): Seawater-basalt interaction at 200°C and 500 bars: implications for origin of sea-floor heavy-metal deposits and regulation of seawater chemistry. *Earth Planet. Sci. Lett.* **25**, 385-397.
- BLACK, A.B. (1953): Broken Hill South mine. In *Geology of Australian Ore Deposits* (A.B. Edwards, ed.). *Austral. Inst. Min. Metall.* **1**, 650-657.
- BOCTOR, N.Z. (1985): Rhodonite solubility and thermodynamic properties of aqueous MnCl₂ in the system MnO-SiO₂-HCl-H₂O. *Geochim. Cosmochim. Acta* **49**, 565-575.
- _____, & FRANTZ, J.D. (1980): Mineral solution equilibria in the system Mn₃O₄-H₂-H₂O-HCl. *Carnegie Inst. Wash. Year Book* **79**, 345-347.
- _____, POPP, R.K. & FRANTZ, J.D. (1980): Mineral-solution equilibria. IV. Solubilities and the thermodynamic properties of FeCl₂ in the system Fe₂O₃-H₂-H₂O-HCl. *Geochim. Cosmochim. Acta* **44**, 1509-1518.
- BONATTI, E., KRAEMER, T. & RYDELL, H. (1972): Classification and genesis of submarine iron-manganese deposits. In *Ferromanganese Deposits on the Ocean Floor* (D. Horn, ed.). Nat. Sci. Foundation, Washington, D.C. (149-165).
- BOSTRÖM, K. & PETERSON, M.N.A. (1969): The origin of aluminum-poor ferromanganoan sediments in areas of high heat flow on the East Pacific Rise. *Mar. Geol.* **7**, 427-447.
- BOTH, R.A. & RUTLAND, R.W.R. (1976): The problem of identifying and interpreting stratiform orebodies in highly metamorphosed terrains: the Broken Hill example. In *Handbook of Stratabound and Stratiform Ore Deposits*, 4 (K.N. Wolf, ed.). Elsevier, Amsterdam (261-325).
- BOWERS, T.S., VON DAMM, K.L. & EDMOND, J.M. (1985): Chemical evolution of mid-ocean ridge hot springs. *Geochim. Cosmochim. Acta* **49**, 2239-2252.
- BRAITHWAITE, R.L. (1974): The geology and origin of the Rosebery ore deposit, Tasmania. *Econ. Geol.* **69**, 1086-1101.
- CORLISS, J.B., MITCHELL, L., DYMOND, J. & CRANE, K. (1978): The chemistry of hydrothermal mounds near the Galapagos rift. *Earth Planet. Sci. Lett.* **40**, 12-24.
- CRERAR, D.A., CORMICK, R.K. & BARNES, H.L. (1980): Geochemistry of manganese: an overview. In *Geology and Geochemistry of Manganese* (I.M. Varentsov & G.Y. Grasslly, eds.). *Akad. Kiado, Budapest* **1**, 293-334.
- DYMOND, J., CORLISS, J.B., HEATH, G.R., FIELD, C.W., DASCH, E.J. & VEEH, H.H. (1973): Origin of metaliferous sediments from the Pacific Ocean. *Geol. Soc. Am. Bull.* **84**, 3355-3372.
- EVERNDEN, J.F. & RICHARDS, J.R. (1961): Potassium-argon ages at Broken Hill, Australia. *Nature* **192**, 446.
- FRANTZ, J.D. & MARSHALL, W.C. (1984): Electrical conductances and ionization constants of salts, acids, and bases in supercritical aqueous fluids: I. Hydrochloric acid from 100° to 700°C and at pressures to 4000 bars. *Am. J. Sci.* **284**, 651-667.
- GEOLOGICAL SUBCOMMITTEE OF THE LATE SCIENTIFIC SOCIETY OF BROKEN HILL (1910): The geology of the Broken Hill lode. *Austral. Inst. Min. Engineers* **15**, 161-263.
- HACKETT, J.P., JR. & BISCHOFF, J.L. (1973): New data on the stratigraphy, extent, and geologic history of the Red Sea geothermal deposits. *Econ. Geol.* **68**, 553-564.
- HAWKINS, B.W. (1968): A quantitative chemical model of the Broken Hill lead-zinc deposit (with discussion). *Austral. Inst. Min. Metall. Proc.* **227**, 11-15.
- HAYDON, R.C. & MCCONACHY, G.W. (1987): The stratigraphic setting of Pb-Zn-Ag mineralization at Broken Hill. *Econ. Geol.* **82**, 826-856.
- HELGESON, H.C. & KIRKHAM, D.H. (1974): Theoretical prediction of the thermodynamic behavior of aqueous electrolytes at high pressures and temperatures. I. Summary of the thermodynamic/electrostatic properties of the solvent. *Am. J. Sci.* **274**, 1089-1198.
- _____, _____ & FLOWERS, G.C. (1981): Theoretical prediction of the thermodynamic behavior of aqueous electrolytes at high pressures and temperatures. IV. Calculation of activity coefficients, osmotic coefficients, and apparent molal and standard and relative partial molal properties to 600°C and 5 kb. *Am. J. Sci.* **281**, 1249-1516.
- HENDERSON, Q.J. (1953): North Broken Hill mine. In *Geology of Australian ore deposits* (A.B. Edwards, ed.). *Austral. Inst. Min. Metall.* **1**, 627-649.
- HICKS, J.A., MOORE, J.M. & REID, A.M. (1985): The co-occurrence of green and blue gahnite in the Namaqualand metamorphic complex, South Africa. *Can. Mineral.* **23**, 535-542.
- HODGSON, C.J. (1975): The geology and geological development of the Broken Hill lode in the New Broken Hill Consolidated mine, Australia. III. Petrology and petrogenesis. *J. Geol. Soc. Aust.* **22**, 195-213.

- HUEBNER, J.S., FLOHR, M.J.K. & JONES, B.F. (1986): geochronological study of the Willyama Complex, Broken Hill, Australia. *J. Petrol.* **8**, 283-324.
- JACQUET, J.B. (1894): Geology of the Broken Hill lode and Barrier Ranges mineral field, N.S.W. *Geol. Surv. New South Wales Mem.* **5**, 1-149.
- JOHNSON, I.R. & KLINGNER, G.D. (1975): Broken Hill ore deposit and its environment. In *Economic Geology of Australia and Papua New Guinea. 1. Metals* (C.L. Knight, ed.). *Austral. Inst. Min. Metall. Mon.* **5**, 476-491.
- JONES, T.R. (1968): Garnet sandstones and garnet rims at orebody contacts, Broken Hill. In *Broken Hill Mines-1968* (M. Radmanovich & J.T. Woodcock, eds.). *Austral. Inst. Min. Metall., Mon.* **3**, 171-178.
- LAING, W.P., MARJORIBANKS, R.W. & RUTLAND, R.W.R. (1978): Structure of the Broken Hill mine area and its significance for the genesis of the orebodies. *Econ. Geol.* **73**, 1112-1136.
- _____, SUN, S.S. & NESBITT, R.W. (1984): Acid volcanic precursor to Potosi gneiss at Broken Hill and its implications for ore genesis. *Seventh Aust. Geol. Conv.*, 318-320 (abstr.).
- LEE, S.D. (1977): Metasomatic alteration associated with the Broken Hill orebody, N.S.W. *Second Aust. Geol. Conv.*, 45 (abstr.).
- MAIDEN, K. (1972): *Studies on the Effects of High Grade Metamorphism on the Broken Hill Orebody*. Ph.D. thesis, Univ. New South Wales, Sydney, Australia.
- McKAY, A.D. (1974): *Variations in the Orebody and Mine Sequence at the Extremities of the Lead Lode, Broken Hill*. M.S. thesis, Univ. Sydney, Sydney, Australia.
- MORGAN, J.J. (1967): Chemical equilibria and kinetic properties of manganese in natural waters. In *Principles and Applications of Water Chemistry* (S.D. Faust & J.V. Hunter, eds.). John Wiley & Sons, New York (561-624).
- MOTTL, M.J., HOLLAND, H.D. & CORR, R.F. (1979): Chemical exchange during hydrothermal alteration of basalt by seawater. II. Experimental results for Fe, Mn, and sulfur species. *Geochim. Cosmochim. Acta* **43**, 869-884.
- O'DRISCOLL, E.S. (1953): The Zinc Corporation and the New Broken Hill Consolidated mines. In *Geology of Australian Ore Deposits* (A.B. Edwards, ed.). *Austral. Inst. Min. Metall.* **1**, 658-673.
- PIDGEON, R.T. (1967): A rubidium-strontium geochronological study of the Willyama Complex, Broken Hill, Australia. *J. Petrol.* **8**, 283-324.
- PLIMER, I.R. (1976): Garnet-biotite relationships in high grade metamorphic rocks at Broken Hill, Australia. *Geol. Mag.* **113**, 263-270.
- _____. (1979): Sulphide rock zonation and hydrothermal alteration at Broken Hill., Australia. *Inst. Min. Metall. Trans.* **B88**, 161-176.
- _____. (1985): Broken Hill Pb-Zn-Ag deposit - A product of mantle metasomatism. *Miner. Deposita* **20**, 147-153.
- _____. & LOTTERMOSER, B.G. (1988): Comment and reply on "Sedimentary model for the giant Broken Hill Pb-Zn deposit, Australia". *Geology* **16**, 564-568.
- RANSOM, D.M. (1969): *Structural and Metamorphic Studies at Broken Hill*. Ph.D. thesis, Australian National Univ., Canberra, Australia.
- REIMANN, C. & STUMPF, E.F. (1981): Geochemical setting of strata-bound stibnite mineralization in the Kreuzeck Mountains, Austria. *Inst. Min. Metall. Trans.* **B90**, 126-132.
- RICHARDS, J.R. & PIDGEON, R.T. (1963): Some age measurements on micas from Broken Hill, Australia. *J. Geol. Soc. Aust.* **10**, 24-60.
- RICHARDS, S.M. (1966): The banded iron formations at Broken Hill, Australia, and their relationship to the lead-zinc orebodies. *Econ. Geol.* **61**, 257-274.
- ROBIE, R.A., HEMINGWAY, B.S. & FISHER, J.R. (1978): Thermodynamic properties of minerals and related substances at 298.15 K and 1 bar (10^5 pascals) pressure and at higher temperatures. *U.S. Geol. Surv. Bull.* **1452**.
- ROZENDAAL, A. & STUMPF, E.F. (1984): Mineral chemistry and genesis of Gamsberg zinc deposit, South Africa. *Inst. Min. Metall. Trans.* **B93**, 161-175.
- RUSSELL, M.J. (1974): Manganese halo surrounding the Tynagh ore deposit, Ireland: a preliminary note. *Inst. Min. Metall. Trans.* **B83**, 65-66.
- _____. (1983): Major sediment-hosted exhalative zinc + lead deposits: formation from hydrothermal convection cells that deepen during crustal extension. *Mineral. Assoc. Can., Short Course Handbook* **8**, 251-282.
- RYAN, P.J., LAWRENCE, A.L., LIPSON, R.D., MOORE, J.M., PATERSON, A., STEDMAN, D.P. & VAN ZYL, D. (1982): The Aggeney's base metal sulphide deposits,

- Namaqualand, South Africa. *Econ. Geol. Res. Unit. Univ. Witwatersrand, Inf. Circ.* **160**.
- SCOTT, M.R., SCOTT, R.B., RONA, P.A., BUTLER, L.W. & NALWALK, A.J. (1974): Rapidly accumulating manganese deposit from the median valley of the mid-Atlantic ridge. *Geophys. Res. Lett.* **1**, 355-358.
- SEGNI, E.R. (1961): Petrology of the zinc lode, New Broken Hill Consolidated Ltd., Broken Hill, New South Wales. *Austral. Inst. Min. Metall. Proc.* **199**, 87-112.
- SEYFRIED, W. & BISCHOFF, J.L. (1977): Hydrothermal transport of heavy metals by seawater: the role of the seawater/basalt ratio. *Earth Planet. Sci. Lett.* **34**, 71-77.
- SHAW, S.E. (1968): Rb-Sr isotopic studies of the mine sequence rocks at Broken Hill. In Broken Hill Mines - 1968 (M. Radmanovich & J.T. Woodcock, eds.). *Aust. Inst. Min. Metall. Mon.* **3**, 185-198.
- SPRY, P.G. (1978): *The Geochemistry of Garnet-rich Lithologies Associated with the Broken Hill Orebody, N.S.W., Australia*. M.S. thesis, Univ. Adelaide, Adelaide, Australia.
- _____ (1979): Manganese anomalies associated with volcanic exhalative sulfide deposits: the Broken Hill example. *Geol. Assoc. Can. - Mineral. Assoc. Can., Program Abstr.* **4**, 80.
- _____ (1987): The chemistry and origin of zincian spinel associated with the Aggeney's Cu-Pb-Zn-Ag deposits, Namaqualand, South Africa. *Miner. Deposita* **22**, 262-268.
- STANTON, R.L. (1976): Petrochemical studies of ore environment at Broken Hill, New South Wales. **3**. Banded iron formations and sulfide orebodies: constitutional and genetic ties. *Inst. Min. Metall. Trans.* **B85**, 132-141.
- _____ (1982): Metamorphism of a stratiform sulphide orebody at Mount Misery, Einasleigh, Queensland, Australia. **1**. Observations. *Inst. Min. Metall. Trans.* **B91**, 47-71.
- _____, ROBERTS, W.P.H. & CHANT, R.A. (1978): Petrochemical studies of the ore environment at Broken Hill, N.S.W. **5**. Major element constitution of the lode and its interpretation. *Austral. Inst. Min. Metall. Proc.* **266**, 51-78.
- _____ & RUSSEL, R.D. (1959): Anomalous leads and the emplacement of lead sulfide ores. *Econ. Geol.* **54**, 588-607.
- _____ & WILLIAMS, K.L. (1978): Garnet compositions at Broken Hill, New South Wales, as indicators of metamorphic processes. *J. Petrol.* **19**, 514-529.
- STEVENS, B.P.J., STROUD, W.J., WILLIS, I.L., BRADLEY, G.M., BROWNE, R.L. & BARNES, R.G. (1980): A stratigraphic interpretation of the Broken Hill Block. In A Guide to the Stratigraphy and Mineralization in the Broken Hill Block, New South Wales (B.P.J. Stevens, ed.). *Geol. Surv. New South Wales Records* **20**, 9-32.
- STILLWELL, F.L. (1922): The rocks in the immediate neighborhood of the Broken Hill lode and their bearing on its origin. *Geol. Surv. New South Wales Mem.* **8**, 354-396.
- _____ (1959): Petrology of the Broken Hill lode and its bearing on ore genesis. *Austral. Inst. Min. Metall. Proc.* **190**, 1-84.
- STUMPFL, E.F. (1979): Manganese haloes surrounding metamorphic stratabound base metal deposits. *Miner. Deposita* **14**, 207-217.
- TOTH, J.R. (1980): Deposition of submarine crusts rich in manganese and iron. *Geol. Soc. Am. Bull.* **91**, 44-54.
- TRACY, R.J. (1982): Compositional zoning and inclusions in metamorphic minerals. In Characterization of Metamorphism Through Mineral Equilibria (J.M. Ferry, ed.). *Mineral. Soc. Am., Rev. Mineral.* **10**, 355-393.
- VALLIANT, R.I. & BARNETT, R.L. (1982): Manganiferous garnet underlying the Bousquet gold orebody, Quebec: metamorphosed manganese sediment as a guide to gold ore. *Can. J. Earth Sci.* **19**, 993-1010.
- VAUGHAN, J.P. & STANTON, R.L. (1986): Sedimentary and metamorphic factors in the development of the Pegmont stratiform Pb-Zn deposit, Queensland, Australia. *Inst. Min. Metall. Trans.* **B95**, 94-121.
- WILLIS, I.L., BROWN, R.E., STROUD, W.J. & STEVENS, B.P.J. (1983): The Early Proterozoic Willyama Supergroup: stratigraphic subdivision and interpretation of high to low-grade metamorphic rocks in the Broken Hill Block, New South Wales. *J. Geol. Soc. Aust.* **30**, 195-224.
- WONDER, J.D., SPRY, P.G. & WINDOM, K.E. (1988): Geochemistry and origin of manganese-rich rocks related to iron-formation and sulfide deposits, western Georgia. *Econ. Geol.* **83**, 1070-1081.
- WRIGHT, J.V., HAYDON, R.C. & MCCONACHY, G.W. (1987): Sedimentary model for the giant Broken Hill Pb-Zn deposit, Australia. *Geology* **15**, 598-602.

Received October 2, 1987, revised manuscript accepted August 24, 1988.